Proceedings of the 3rd IASME/WSEAS Int. Conf. on FLUID DYNAMICS & AERODYNAMICS, Corfu, Greece, August 20-22, 2005 (pp245-250)

A numerical investigation on vortex breakdown in swirling jets

DARIO AMIRANTE and KAI H. LUO
School of Engineering Sciences
University of Southampton
Highfield, Southampton SO17 1BJ
UNITED KINGDOM
dario@soton.ac.uk, k.h.luo@soton.ac.uk

Abstract: - Direct numerical simulations at a range of Reynolds numbers are performed to investigate mechanism of vortex breakdown in swirling jets. Both axisymmetric and fully three-dimensional simlations are conducted using high-order numerical methods in cylindrical coordinates. Our results clearly indicate vortex breakdown as a wave phenomenon. Our analyses show how the bifurcation diagram found at high Reynolds numbers correlate with the flow field computed and how the behaviour changes at low Reynolds numbers.

Key-Words:- Swirling flows, vortex breakdown, bifurcation diagram

1 Introduction

A commonly accepted definition of vortex breakdown is the abrupt and drastic change of structure which may occur in the vortex core of a swirling flow, when the swirl ratio exceeds a threshold value. In one of the first experimental works on the topic, Harvey [3] describes the phenomenon as the formation of a well confined region of reversed flow with a shape of a body of revolution located on the axis, imposing the approaching flow to move around it.

Several technical applications employ swirl, but the main reason of interest in vortex breakdown arises because of its foundamental mechanism, which seems to be similar to other fluid dynamic phenomena like shock waves and the hydraulic jump. In a swirling flow, even if the stability of the basic flow is guaranteed, the restoring effect of the Coriolis force generates longitudinal inertial waves, the so called Kelvin waves [11]. In the absence of axial velocity, these waves can propagate upstream marginally, with the velocity becoming higher as the swirl is increased. When the axial velocity is not zero, but bigger than the speed of waves propagating upstream, any perturbation is convected downstream by the main flow. For a fixed axial velocity, there exists a critical level of swirl for which an infinitesimal axisymmetric standing wave can be sustained from the base flow [1]. Below the critical level the flow is *supercritical* and waves can only propagate downstream; upstream propagation of energy becomes possible above the critical level, when the flow is said to be *subcritical*.

The critical state is defined for a swirling flow which is assumed to be columnar, extending to infinity both upstream and downstream. In real situations the flow is never uniform, but, due to geometrical contraints and viscous diffusion, it has conditions slowly evolving which may lead an initial supercritical flow towards criticality. Whereas if a critical condition is reached, perturbations spreading from the subsequent subcritical region will accumulate and amplify to large value resulting in a possible breakdown. Leibovich [6], using a weakly non-linear analysis derives the evolution of waves of finite amplitude in a vortex core. The wave amplitude is governed by a Korteweg-de Vries equation, whose solutions are the well known *solitons*, waves of permanent form arising from the non-linear interaction of dispersive waves. The resulting finite wave presents a dependence of the velocity on the amplitude: as it grows it becomes faster and therefore can penetrate the supercritical region, unaccessible for small perturbations. In this scenario, a steady configuration becomes possible only if a mechanism extracting energy from the big wave arises. Experimental works [12] have revealed a very weak sensitivity to viscosity for high Reynolds numbers. Leibovich and Kribus [7] suggest non-axisymmetric feautures, rather than viscosity, as the most dissipative effect helping to stabilize the wave.

This mechanism would provide some insights into the histeretical behaviour that unsteady axisymmetric simulations reveal for large Reynolds numbers (Re$\geq$300) [4],[8]: some quantities, like the minimum axial velocity, when represented as func-

tion of the swirl level, show multiple steady solutions. Figure (1) illustrates a schematic representation of the minimum axial velocity W obtained for different values of the swirl. Here we remark that W$\leq$ 0 indicates breakdown. Starting from a condition with low swirl the solution moves along the branch (I), corresponding to a quasi-columnar configuration until the first folding point S1 is reached. For S>S1 solution evolves towards branch (II) and a stagnation point appears. At this stage, a successive reduction of swirl below the critical value S1 is unable to restore the initial quasi-columnar configuration until a second folding point S2 is reached.

This behaviour is connected to bifurcating solutions of the *steady* Navier-Stokes equations. Wang and Rusak [14] apply a global variational approach to the inviscid Rankine vortex in a pipe, and derive a bifurcation diagram which resembles the viscous results found by numerical computations. In particular they prove the existence of the two limit points S1 and S2 such that for S1<S<S2 three solutions exist: solutions on branch (I) representing a columnar flow; solutions on branch (II) representing a well localized region of separated flow; there exists a third branch (III), connecting the two folding points, which describes waves developing in the main flow. This branch is unstable and cannot be obtained as steady solution of a time marching calculation, but could be found using a steady state case in combination with continuation techniques [2].

The numerical computations of Beran [2], Lopez [8] and Herrada *et al.* [4] are seen as a viscous correction of the these results. S1 is the critical point for infinitesimal disturbance, while S2 is believed to be a critical state for *finite amplitude* waves [14]. When the Reynolds number is high enough, the flow becomes locally critical, non-linear waves interact and propagate upstream; in the inviscid limit the only mechanism which may trap the large wave is due to the boundary conditions fixed at the inlet. For moderate Reynolds numbers the dissipative effect of viscosity is no longer negligible, and the large wave can come to rest before approaching the inlet. The corresponding bifurcation diagram is modified and the third branch becomes shorter up to disappear.

In this work, we have carried out a fairly extensive numerical investigation of compressible swirling flows in open domains. The main object of the study was to determine numerically the bifurcation diagram and see how it correlates with the flow field computed. We have analyzed the relation between the existence of branch (II) and the excursion of the vortex bubble. Furthermore,

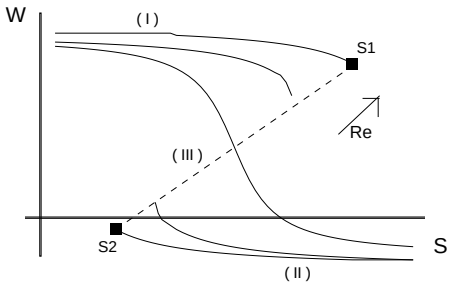

Figure 1: Typical bifurcation diagram

a fully three-dimensional case is presented to highlight how non-axisymmetric features can develop.

2 Problem formulation

In the present investigation we study the evolution of a vortex whose non-dimensional components in cylindrical coordinates (r, θ, z) are

$$\begin{aligned} V_\theta &= \begin{cases} Sr(2-r^2) & 0 \leq r \leq 1 \\ S/r & r \geq 1 \end{cases} \\ V_z &= 1 \\ V_r &= 0 \end{aligned} \tag{1}$$

where the vortex core radius $\overline{L}$ and the uniform axial velocity $\overline{V_z}$ have been used as reference dimensional quantities. The swirl number S is the ratio between the azimuthal velocity at the vortex radius and the axial velocity. These velocity profiles have been recently investigated by Ruith *et al.* [10] for incompressible flows. The thermodynamic initial conditions are the following: density is assumed constant in all the domain and pressure is fixed to satisfy the radial momentum equation. The reference density is the constant free-stream density, the reference pressure is twice the dynamic pressure at the inflow and the reference temperature is the temperature on the axis at the inflow, thus we obtain:

$$\begin{aligned} \rho &= 1 \\ T &= \gamma M_\infty^2 p \\ \frac{\partial p}{\partial r} &= \frac{V_\theta^2}{r} \end{aligned} \tag{2}$$

where M_∞ is the Mach number on the axis at the inlet. The computational domain has the dimensions R=8 and Z=16. To reflect the physical situation of a jet in an open domain, density and velocity are kept constant at the inflow boundary according to (1) and (2); non-reflective conditions are

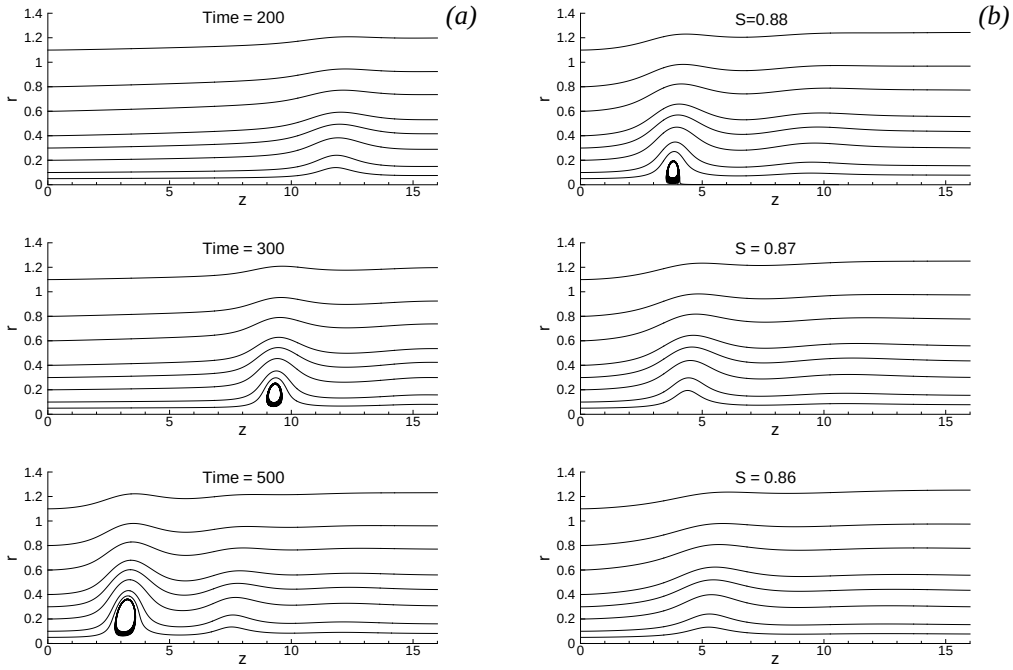

Figure 2: Re=400 case. *(a):* Evolution of istantaneous streamlines at $S = 0.9$. *(b):* Streamlines for steady solutions found on branch (II).

applied at the open sides and, in the axisymmetric calculations, a symmetric boundary is imposed on the axis.

3 Numerical method

A finite difference method has been used to solve the unsteady, compressible Navier-Stokes equations in cylindrical coordinates. The spatial discretization is performed using the sixth order Lele's compact scheme [5] for the axial and radial direction, while, in the three-dimensional calculations, derivatives in the periodical direction are obtained with a spectral method employing a FFT algorithm. In order to obtain a better representation of the higher wave numbers and to improve the numerical stability, all the viscous terms requiring evaluation of successive derivatives, for example the terms

$$\frac{\partial}{\partial r}\left[\mu\frac{\partial V_r}{\partial r}\right]$$

have been expanded and evaluated like:

$$\frac{\partial \mu}{\partial r}\frac{\partial V_r}{\partial r} + \mu\frac{\partial^2 V_r}{\partial r^2}$$

Equations are explicitly integrated in time by a fourth order low-storage Runge-Kutta method [15]. Boundary conditions are treated with the NSCBC formulation of Poinsot and Lele [9] with viscous corrections. We didn't use any stretching of the grid in order to preserve the overall high accuracy of the scheme. For the three-dimensional simulations, the grid is staggered to avoid the singularity on the axis and in order to alleviate the CFL time step restriction, azimuthal normal modes taken for the spectral derivatives are dropped when approaching the axis. Table 1 reports the grid resolution requirements at different Reynolds numbers to obtain a reasonable good grid convergence.

Re	n_z	n_r	n_θ
200	201	161	64
400	251	161	-
1000	351	251	-

Table 1: Grid resolution for different Reynolds numbers

4 Results and discussion

We discuss results from three different Reynolds numbers, namely Re=200, 400 and 1000. The Mach number is $M_\infty = 0.5$. For each case treated, branch

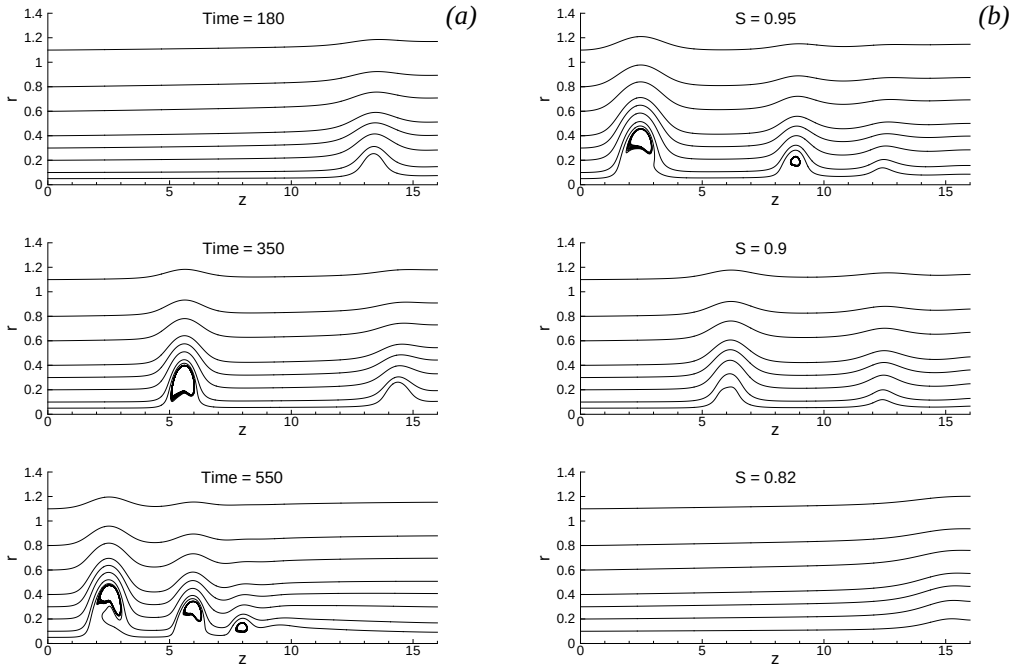

Figure 3: Re=1000 case. *(a):* Evolution of istantaneous streamlines at $S = 1$. *(b):* Streamlines for steady solutions found on branch (II).

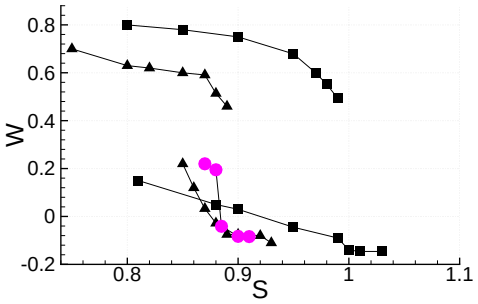

Figure 4: Computed bifurcation diagram at Re=1000 (squares), Re=400 (triangles) and Re=200 (circles)

(I) of the bifurcation diagram is obtained by increasing the swirl number until a stagnation point appears. Branch (II) is then derived assuming the steady state solution at S=S1 as initial condition for a new run with a slightly smaller value of S. The process is then iterated until the quasi-columnar configuration is established again. The computed bifurcation diagram is presented in figure 4. For Re=400 the quasi-columnar configuration is lost at S=0.9. When this level of swirl is reached, the flow evolves as shown in figure 2-*a*. Here the istantaneous streamlines on a meridian plane are plotted at different times. The inflow is on the left side. The perturbation arises close to the outflow boundary, then it moves upstream growing in amplitude and leading to a region of separeted flow at approximately Time=300. A final quasi-steady configuration is reached at Time=500 with the vortex bubble located in proximity of the inlet where the velocity is kept fixed and no wave motion is possible. A similar process develops for Re=1000 (fig. 3-*a*) . Here, as the first wave moves upstream, an other wave takes place in the wake of it and the final quasi-steady state presents a wave train superimposed to the main flow. In this case the amount of swirl necessary to breakdown the vortex is much higher. This is consistent with the role played by viscous diffusion, which is the driving element leading the initial supercritical flow towards a local criticality. For the same reason, not only in the two mentioned cases, but in all the simulations carried on at moderate high Reynold numbers, we have found that the perturbation leading to breakdown always begins to develop close to the outlet boundary.

This feauture ceases to exist at low Reynolds numbers (Re $\leq$ 200) for which the whole process apparently seems to lose the connotations of wave phenomenon (see fig. 5); the perturbation builds up far from the outlet boundary and no upstream

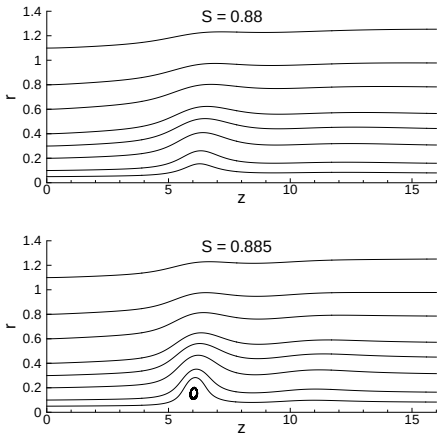

Figure 5: Re=200 case. Streamlines for steady solutions. The bubble is trapped where it develops.

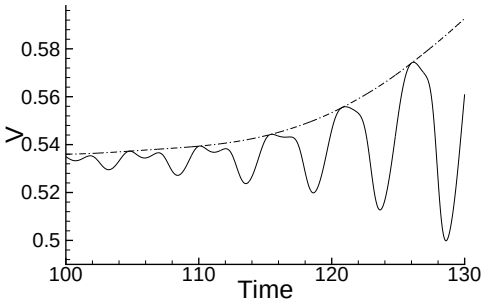

Figure 6: Time evolution of V_θ at θ =0, r=0.1, z=8 (solid line) and of maximum value of the function $V_\theta(r)$ at r=0.1, z=8 (dash line)

migration exists.

Now we investigate the flow behaviour when the swirl number is sequentially decreased below the critical value. For the Re=400 case, (see fig. 2-*b*) the bubble becomes smaller and moves slightly upstream at S=0.88. The region of reversed flow disappears at S=0.87, however a well pronounced swelling of the streamlines is still present, indicating that although there's no breakdown, a wave of finite amplitude is still localized. The wave becomes weaker as the swirl is decreased and undergoes a small shift of its axial position before disappearing. The Re=1000 case (fig. 4-b) is more interesting because it clearly shows the wave convected downstrem from the main flow. When the second folding point S2=0.82 is reached, a light swelling is located exactly at the outlet, thus the re-establishment of the columnar configuration is associated to the expulsion of the wave from the computational domain. We believe this case to be

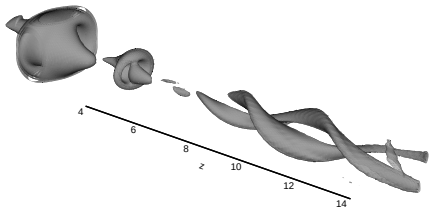

Figure 7: Iso-surface of azimuthal vorticity component. Re=200, S=1.095

quite well representative of the inviscid limit analyzed theoretically by Wang and Rusak [14]. When the swirl is decreased below the critical value S1 the main flow reduces its capibility to sustain waves and the vortex bubble is pushed away weakened. In a process where the dissipative effects of viscosity are negligible one expects the wave resulting from the downstream migration to be located where it was initially originited when the first point S1 had been reached. Viscosity renders the process unreversible: for intermediate Reynolds numbers the bubble can reach the inlet at S=S1 but not the outlet at S=S2 while at low Reynolds numbers the viscous diffusion can be so high to trap the wave where it's formed. The existence of multiple steady solutions seems therefore associated to the *downstream* excursion of breakdown, and different solutions on branch (II) represent a standing wave positioned at different axial positions.

The flow behind the vortex bubble presents a wake-like behaviour which is expected to undergo helical vortex shedding arising from linear instability. Previous works of Tromp and Beran [13], Ruith *et al.* [10] show that the mechanism leading to breakdown is essentially axisymmetric, however vortex breakdown found in experimental works [12] generally presents non axisymmetric forms, the so called spiral and double spiral forms. In our work we have used axisymmetric steady solutions obtained at Re=200 as initial conditions for fully three-dimensional simulations. A random perturbation in the azimuthal component of velocity has been introduced at the inflow for the only first iteration. Figure 6 illustrates the temporal evolution of azimuthal velocity component at the location θ =0, r=0.1, z=8 for the S=1.095 case. The signal exhibits a trend of the form

$$e^{\sigma t} cos(\omega t - m\theta)$$

where the selected mode m is found to be 1 from the spectral analysis of the function $V_\theta = V_\theta(\theta)$ at Time=130. On the same figure is also plotted the maximum azimuthal component for $0 \leq \theta \leq 2\pi$ at the same axial and radial station. This curve coincides with the envelope of the V_θ(t) signal, indicating that as the instability takes place, the growing perturbation travels in the azimuthal direction with a period of approximately T=6. The iso-surface of the azimuthal vorticity component confirms the wave number selection of m=1 (fig. 7). We have found the flow stable at Re=100 while the linear growth rate found at Re=200 , with S=0.95 and S=1.095 agrees well with the incompressible results of Ruith [10], suggesting a small dependence on compressibility. In particular the case Re=200 S=1.095 is expected to be a limit point above which higher modes can be selected and the double-helix structure of breakdown can develop. This point is under investigation.

5 Conclusions

As reported in [7], the main elements underlying vortex breakdown phenomenon are: *(a)* large-amplitude axisymmetric waves, *(b)* three-dimensional instabilities of small amplitude. Both the elements are revealed in our numerical computations. In particular, we have tried to emphasize how the histeretical behaviour found at high Reynold numbers can be explained in terms of the vortex bubble motion.

In summary, our results support the idea that multiple steady solutions exist when the vortex bubble is so "strong" to be able to migrate upstream when the level of swirl is reduced under the critical point S1. In this case, solutions on branch (II) of the bifurcation diagram represent standing waves localized at different axial positions. The critical point S2 represents *always* a small wave. It will be located in proximity of the outlet boundary if the Reynolds number is high enough, while its axial position moves away from it as the dissipative effect of viscosity increases. The highest Reynolds number in correspondence of which the vortex bubble is unable to move downstream represents the limit point when the bifurcation diagram loses branch (II) and multiple solutions disappear.

References

[1] Benjamin B., Theory of the vortex breakdown phenomenon, *J. Fluid Mech.*, Vol.14, 1962, pp. 593-629.

[2] Beran P.S. and Culik F.E.C., The role of nonuniqueness in the development of vortex breakdown in tubes, *J. Fluid Mech.*, Vol.242, 1992, pp. 491-527.

[3] Harvey J.K., Some observations of the vortex breakdown phenomenon, *J. Fluid Mech.*, Vol.14, 1962, pp. 585-592.

[4] Herrada M.A., Perez-Saborid M. and Barrero A., Vortex breakdown in compressible flows in pipes, *Phys. Fluids*, Vol.15, 2003, pp. 2208-2218.

[5] Lele S.K., Compact finite differences schemes with spectral-like resolution, *J. Comput. Phys.*, Vol.103, 1992, pp. 16-42.

[6] Leibovich S., Weakly non-linear waves in rotating fluids, *J. Fluid Mech.*, Vol.42, 1970, pp. 803-822.

[7] Leibovich S. and Kribus A., Large-amplitude wavetrains and solitary waves in vortices, *J. Fluid Mech.*, Vol.216, 1990, pp. 459-504.

[8] Lopez J.M., On the bifurcation structure of axisymmetric vortex breakdown in a constricted pipe, *Phys. Fluids*, Vol.6, 1994, pp. 3683-3693.

[9] Poinsot T.J. and Lele S.K., Boundary conditions for direct simulations of compressible viscous flows, *J. Comput. Phys.*, Vol.101, 1992, pp. 104-129.

[10] Ruith M.R., Chen P., Meiburg E. and Maxworthy T., Three-dimensional vortex breakdown in swirling jets and wakes: direct numerical simulations, *J. Fluid Mech.*, Vol.486, 2003, pp. 331-378.

[11] Saffman P.G., *Vortex Dynamics*, Cambridge University Press, 1992

[12] Sarpkaya T., On stationary and travelling vortex breakdown, *J. Fluid Mech.*, Vol.45, 1971, pp. 545-559

[13] Tromp J.C. and Beran P.S., The role of nonunique axisymmetric solutions in 3-D vortex breakdown, *Phys. Fluids*, Vol.9, 1997, pp 992-1002

[14] Wang S. and Rusak Z., The dynamics of a swirling flow in a pipe and transition to axisymmetric vortex breakdown, *J. Fluid Mech.*, Vol.340, 1997, pp. 177-223

[15] Williamson J.H., Low-storage Runge-Kutta schemes, *J. Comput. Phys.*, Vol.35, 1980, pp.45-56